

The effect of nickel on the martensitic-type transformations of Pt₃Al and TiPt

T. Biggs, L.A. Cornish¹, M.J. Witcomb² and M.B. Cortie

Physical Metallurgy Division, Mintek, Private Bag X3015, Randburg 2125, South Africa

¹ *School of Process Engineering, University of Witwatersrand, Private Bag 3, Wits 2050, South Africa*

² *Electron Microscope Unit, University of Witwatersrand, Private Bag 3, Wits 2050, South Africa*

Abstract: The effect of nickel on two classes of martensitic-type transformations in platinum systems has been studied. The first transformation is L1₂ to DO_c' in the Pt₃Al system and the second is B2 to B19 in the TiPt system. The microstructures after transformation in the two systems are very different. The product of the Pt₃Al transformation has a twinned microstructure, typical of cubic-to-tetragonal transformations. The product of the TiPt transformation is lath-like, although the morphology can be altered using heat treatments. The parent phase in the TiPt system is not retained at room temperature, whereas the parent phase in the Pt₃Al transformation can be stabilised to room temperature. A great variation in hardness and transformation temperature is seen in each system as the composition is varied about the stoichiometric ratio, which has the lowest hardness. The Pt₃Al transformation temperature has been reported to range from around room temperature to 1000°C. The TiPt transformation temperature can range from 1000 to 1080°C. The effect of nickel additions on these alloys also has a marked effect on the parent and product phase stability, and hence the microstructure and resulting hardness. The effect on the Pt₃Al phase is complex, as nickel appears to stabilise the parent phase. The hardness varied in the region of 350 to 500 HV₁₀. For the TiPt phase, the hardness values were generally found to increase with the nickel additions increasing from 250 to about 600 HV₁₀. The addition of 20 at.% nickel decreases the transformation temperature from around 1000°C to about 600°C.

1. INTRODUCTION

Many different types of martensite transformations have been observed in non-ferrous systems, and some of these systems, have the potential to exhibit shape memory effects. Most existing commercial shape memory alloys (SMAs) function between -100°C and +200°C. However, there is a need for shape memory alloys that can transform reversibly at higher temperatures, for applications such as jet engines. Such alloys are likely to be based on the noble and/or the refractory metals, or a combination of them. Platinum, due to its high melting point and stability, is one such candidate.

Two different classes of martensite-type transformation [1] occur in the platinum-aluminium and platinum-titanium systems. Pt₃Al (Figure 1) exhibits a cubic (L1₂) to tetragonal (DO_c') transformation (tetragonal distortions), while TiPt (Figure 2) shows a cubic (B2) to orthorhombic (B19) transformation. Discrepancies exist in the literature with regard to the transformation temperatures of the Pt₃Al system, which is reported to vary with composition from room temperature to either 400°C [2] or to 1000°C [3]. The transformation of the TiPt phase occurs around 1000°C, making it very promising for high temperature SMA applications [4].

The effect of nickel on both these transformations is the subject of the present investigation. Since TiNi is a commercial shape memory alloy which exhibits a cubic (B2) to monoclinic (B19') transformation, it was hoped that nickel would stabilise the martensite transformations in the ternary systems.

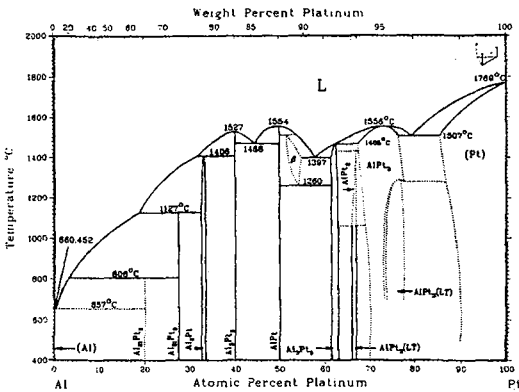


Figure 1: Al-Pt phase diagram [3].

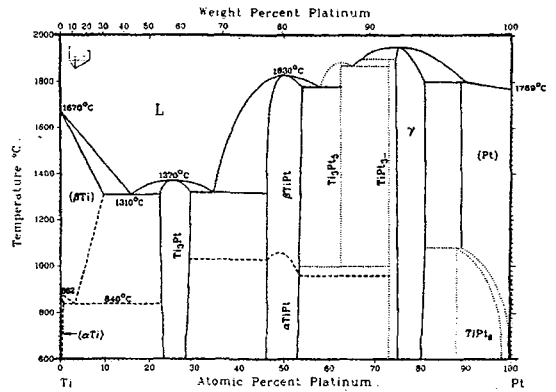


Figure 2: Ti-Pt phase diagram [3].

2. PLATINUM-ALUMINIUM-NICKEL SYSTEM

A martensite-type transformation occurs around 75 at.% platinum as the structure changes from a high temperature cubic Pt_3Al structure ($L1_2$, ordered fcc, HT) to a low temperature tetragonal Pt_3Al structure (DO_{19} , ordered fct, LT). The microstructure after the transformation was highly twinned (Figure 3). A range of samples with nickel additions (Table 1) was examined. Microstructural studies were conducted using light microscopy, scanning electron microscopy (SEM) with energy dispersive X-ray analysis facilities (EDS), and X-ray diffraction (XRD). The phase results are summarised in Table 1 and Figure 4. Nickel did not appear to have any effect on the martensitic product, but did stabilise the parent phase, which extended significantly into the ternary. Samples in the platinum-rich region (IN1-IN3 in Table 1) generally lay in a two-phase region of platinum-rich solid solution and LT Pt_3Al phase. Where a significant amount of LT Pt_3Al phase was present, fine twins (about a micrometre in width) were observed within this phase. The addition of nickel made the twins less discernable. Samples consisting of the HT Pt_3Al phase (IL2-IL3) were generally featureless, as in the binary alloys. A two-phase region of HT Pt_3Al phase and (Ni,Pt) solid solution was observed in the ternary (Figure 4). Highly twinned microstructures (Figure 5) were observed in three samples (QA1, QA3 and IL4) at higher aluminium contents than the HT Pt_3Al phase field. The morphology was similar to that observed from the Pt_3Al HT to Pt_3Al LT transformation. Sample IL4 was composed of the twinned phase and a NiPt_2Al (Heusler type) phase (Figure 6). The NiPt_2Al phase was confirmed by XRD modelling. From the composition of the sample and XRD results, it seems unlikely that these twinned microstructures originated from the Pt_3Al HT to Pt_3Al LT martensite-type transformation. It is possible that the twins were derived from a $(\text{NiPt})_2\text{Al}$ structure, but twinning was not observed in the Pt_2Al binary phase [5]. This structure could be due to a $(\text{Ni,Pt})_3\text{Al}$ HT to $(\text{Ni,Pt})_2\text{Al}$ transformation (with the composition remaining unchanged since both phase fields are wide and overlap each other, albeit at different temperatures) that is displacive in nature and observed only in the ternary.

Table 1: Observations for Pt-Al-Ni alloys heat-treated at 1350°C for 3 days, followed by a furnace cool.

Pt (at.%)	Al (at.%)	Ni (at.%)	sample name	Crystal structure (XRD)	Microstructural observations	Hardness (HV _{0.05})
75.3	20.5	4.2	IN1	Low temperature Pt ₃ Al	Twinned Pt ₃ Al + eutectic	391±10
80.2	14.9	4.9	IN2	Low temperature Pt ₃ Al	Pt ₃ Al + eutectic	379±9
75.9	18.5	5.6	IN3	Low temperature Pt ₃ Al	Pt ₃ Al + eutectic	387±6
70.7	24.6	4.7	IL2	High temperature Pt ₃ Al	Single phase Pt ₃ Al (large grains)	421±17
66.4	24.0	9.6	IL3	High temperature Pt ₃ Al	Single phase Pt ₃ Al (large grains)	466±12
55.8	24.3	19.9	IL4	NiPt ₂ Al (Heusler) and second phase of possibly either Pt ₂ Al or Pt ₃ Al	Grey Pt ₂ AlNi matrix + twinned white phase	594±43
63.7	25.2	11.1	QA1	High temperature Pt ₃ Al phase or Pt ₂ Al	Twinned single phase	588±12
69.2	28.4	2.4	QA3	Pt ₂ Al or high temperature + extra peaks	Twinned single phase	591±8
75.5	15.7	8.8	QA4	High temperature Pt ₃ Al	Pt ₃ Al + (Pt), no twins	382±11
69.6	15.9	14.5	QA5	High temperature Pt ₃ Al + (Pt)	Pt ₃ Al + (Pt), no twins	421±7
62.0	15.3	22.7	QA6	High temperature Pt ₃ Al + (Pt)	Pt ₃ Al + (Pt), no twins	536±6

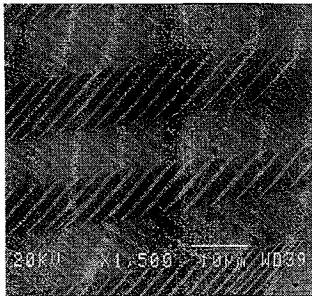


Figure 3: Scanning electron micrograph, in backscattered mode, showing the twinned microstructure of a 75.1 at.% Pt-Al alloy after heat treating at 1350°C for 3 days, followed by a 12 hour furnace cool.

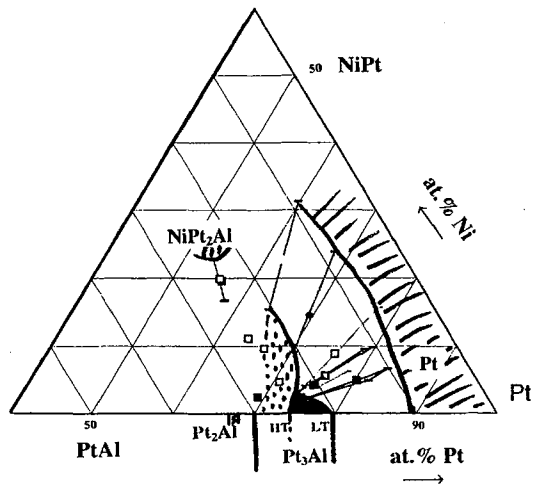


Figure 4: Partial ternary section of the Ni-Pt-Al system. All alloys were heat treated at 1350°C for 3 days, and then furnace cooled.



Figure 5: Light micrograph of a 11.1Ni-63.7Pt-25.2Al alloy after heat treatment at 1350°C for 3 days, followed by a furnace cool.

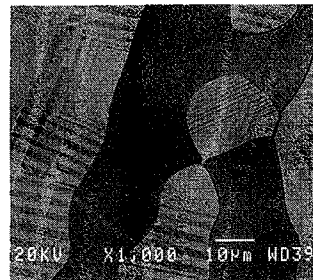


Figure 6: Scanning electron micrograph, in backscattered mode, showing a 19.9Ni-55.8Pt-24.3Al alloy (IL4) after heat treating at 1350°C for 3 days, followed by a furnace cool. The dark phase is NiPt₂Al.

3. PLATINUM-TITANIUM-NICKEL

In the platinum-titanium system a transformation from a B2 structure to a B19 (orthorhombic) structure has been observed around 50 at.% Pt [4,5,6]. The transformation temperature and hardness values vary with composition. In the binary system, the morphology of the B19 TiPt phase was found to depend on the cooling rate after heat treatment (Figures 7 and 8). The effect of nickel has been reported to generally decrease the M_s (Figure 9) [6,7]. The transformation temperatures were measured using differential thermal analysis and showed excellent correlation with Lindquist et al. [7] who investigated samples of 20 at.% Ni and greater (Figure 9). For nickel additions between 5.8-10 at.% (BAN4, BAN5), a second phase was observed (Figure 10). It was unclear whether this lath-like phase was related to the martensite-type transformation. The system was investigated further in an attempt to assess the phase stability of the B19 TiPt phase after nickel additions. The SEM-EDS results are summarised in Table 2 and Figure 11. Minor additions of nickel, less than 5.8 at.%, did not significantly alter the lath-like morphology observed after etching.

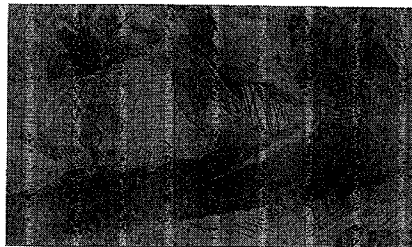


Figure 7: Light micrograph of a 50 at.%Ti-Pt alloy after heat treatment at 1200°C for 3 days, followed by water quench.

Figure 8: Light micrograph of a 50 at.% Ti-Pt alloy after heat treatment at 1200°C, followed by a furnace cool.

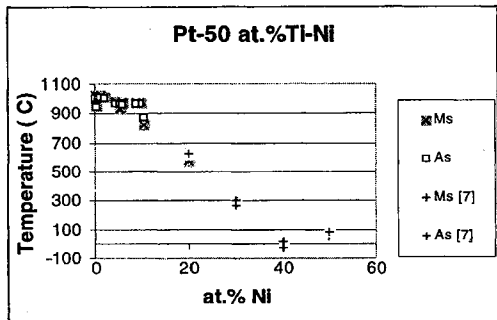


Figure 9: M_s of the TiPt phase with nickel substituting for platinum in the Pt-Ti-Ni system [6,7].

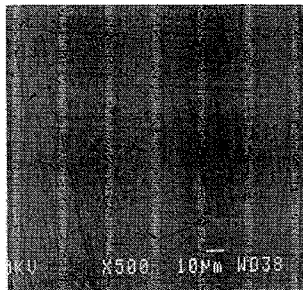


Figure 10: Scanning electron micrograph, in backscattered mode, of a 46.1Ti-10Ni-43.9Pt alloy after heat treatment at 1200°C for 3 days, followed by a furnace cool.

The B19 TiPt orthorhombic phase was found to extend up to about 20 at.% Ni in the ternary, and nickel substituted for platinum. No evidence of a cubic B2 or monoclinic B19' TiNi phase was found. Some ternary additions, such as rhenium, have been observed to stabilise the B2 TiPt phase and, in fact, at higher platinum contents, a two-phase region of B2 TiPt and B19 TiPt has been observed [6]. This would imply diffusion is necessary for the transformation, which would render the transformation non-martensitic. Examination of these results suggests that the Ti_3Pt_5 structure extends into the ternary, at least 10 at.% Ni, and that there is a two-phase B19 TiPt and Ti_3Pt_5 region. The Ti_3Pt_5 phase is orthorhombic and the morphology is plate-like. At higher nickel contents (20 at.%), it is uncertain whether the phase is an extension of Ti_3Pt_5 or an unreported ternary phase. The B2 TiPt parent structure did not account for all the extra peaks observed by XRD, so it is unlikely that this phase was present. There is a grey lath-like phase (Figure 12) similar to that seen for the 10 at.% Ni (BAN5) sample. The XRD spectra are quite similar for the samples, and due to preferred orientations, often difficult to interpret.

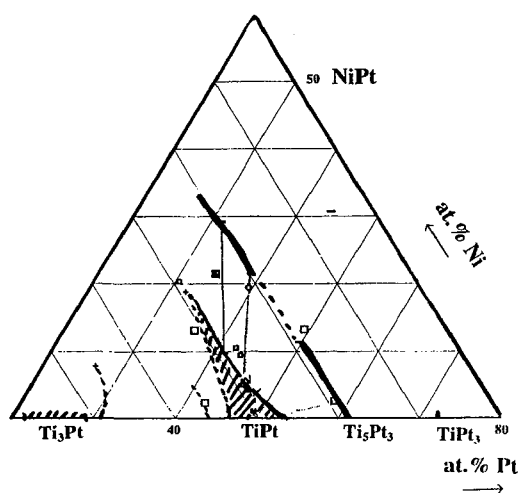


Figure 11: Partial ternary section of Pt-Ti-Ni system. All alloys were heat treated at 1200°C for 3 days, followed by a furnace cool.

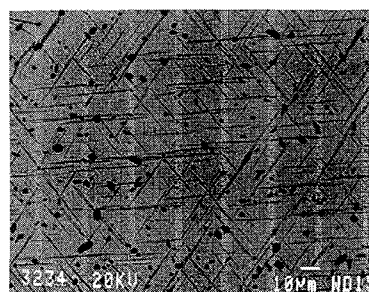


Figure 12: Scanning electron micrograph, in backscattered mode, of a 49.5Ti-20.2Ni-30.3Pt alloy after a heat treatment at 1200°C for 3 days, followed by a furnace cool.

Table 2: Observations for Pt-Ti-Ni alloys heat-treated at 1200°C for 3 days, followed by a furnace cool.

Pt (at.%)	Ti (at.%)	Ni (at.%)	Sample name	Crystal structure (XRD)	Microstructural observations	Hardness (HV _{0.05})
49.1	49.8	1.1	BAN1	B19 TiPt	Lath-like	256±16
48.5	49.3	2.2	BAN2	B19 TiPt	Lath-like	275±20
46.7	49.0	4.3	BAN3	B19 TiPt	Lath-like	319±14
45.9	48.3	5.8	BAN4	B19 TiPt + possibly Ti_3Pt_5	Lath-like, TiPt matrix + grey laths	351±16
43.9	46.1	10.0	BAN5	B19 TiPt + possibly Ti_3Pt_5	Lath-like, TiPt matrix + grey laths	461±12
45.8	48.8	5.4	RTN2	B19 TiPt	Fine grey laths in light matrix + dark grain boundary phase	328±14
39.8	49.8	10.4	RTN3	B19 TiPt	Fine grey laths in light matrix + dark grain boundary phase	382±20
30.3	49.5	20.2	RTN1	Distorted B19 TiPt	Fine grey laths in light matrix + dark grain boundary phase	422±8
36.0	51.0	13.0	QN1	B19 TiPt	Grey matrix plus white needle-like phase + round dark precipitates	457±17
42.5	55.1	2.4	QN2	Ti_3Pt + (TiPt or ?)	Light matrix + grey needle-like phase + large dark phase	571±24
49.4	37.5	13.1	QN3	Possibly Pt_5Ti_3 + ?	Matrix + grey "Chinese script" second phase	380±17
58.3	39.1	2.6	QN4	B19 TiPt + Ti_3Pt_5	Light matrix + dark phase + grey phase	383±35
34.4	44.1	21.5	QN5	B19 TiPt + possibly Ti_3Pt_5 or B2 TiPt?	Dark phase + white needle-like mix	353±12
50.6	49.4	0	LS2	B19 TiPt	Twinned (morphology depends on cooling)	252±15

4. CONCLUSIONS

The low temperature (LT) tetragonal Pt₃Al phase showed a high degree of twinning. With nickel additions, twins were not easily discernable in the LT Pt₃Al phase. A two phase region of the HT Pt₃Al phase (not twinned) and Pt-rich solid solution extended into the ternary. Highly twinned microstructures were also observed at higher aluminium contents in the ternary (around the Pt₂Al phase field). The microstructures were not thought to originate from the transformation of cubic Pt₃Al to tetragonal Pt₃Al. A two-phase region included the NiPt₂Al (Heusler type) phase. Nickel additions generally increased the hardness and appeared to stabilise the parent HT Pt₃Al phase.

The morphology of the martensite-like phase in the Pt-Ti system was more lath-like, and depended on cooling rate. The orthorhombic TiPt B19 phase field extended significantly into the ternary with nickel being substituted for platinum. For low additions of nickel (below 5.8 at.%), the morphology was unchanged. The addition of nickel was found to decrease the transformation temperature and tended to increase the hardness. A two-phase region of the orthorhombic TiPt phase and plate-like Ti₃Pt₅ extended into the ternary. At higher nickel contents, a two-phase region existed, but it is uncertain whether the phase within the ternary was an extension of the Ti₃Pt₅ phase or an hitherto unreported ternary phase.

Acknowledgements

The authors would like to acknowledge the assistance of P. Ellis, I. Klingbiel and support from Mintek and the Microstructural Studies Research Programme at the University of Witswatersrand.

REFERENCES

1. L. Delaey, K. Mukherjee, M. Chandrasekaran, in *Proceedings of the Course: The Science and Technology of Shape Memory Alloys*, Barcelona, edited by J.M. Guilemany, EEC-Comett 87, C-2, 00863, 1989, p.117.
2. Y. Oya, Y. Mishima, T. Suzuki, *Z. Metallkde*, **78**, 485 (1987).
3. T.B. Massalski, *Binary Phase Diagrams*, American Society of Metals, Ohio, USA, (1987).
4. H.C. Donkersloot, J.H.N. Van Vucht, *J. Less-Common Metals*, **20**, 83 (1970).
5. T. Biggs, PhD thesis, University of Witswatersrand (to be submitted).
6. T. Biggs, M.J. Witcomb, L.A. Cornish, *Mater. Sci. Eng. A*, **273-5**, .204 (1999).
7. P.G. Lindquist, C.M. Wayman, *Engineering Aspects of Shape Memory Alloys*, edited by T.W. Duerig, et al., Butterworth-Heinemann Ltd, London, (1990).